JOURNAL OF THE AMERICAN CHEMICAL SOCIETY

Article

pubs.acs.org/JACS

Layered Perovskite Oxide: A Reversible Air Electrode for Oxygen Evolution/Reduction in Rechargeable Metal-Air Batteries

Tatsuya Takeguchi,*,† Toshiro Yamanaka,† Hiroki Takahashi,† Hiroshi Watanabe,† Tomohiro Kuroki,† Haruyuki Nakanishi,‡ Yuki Orikasa,§ Yoshiharu Uchimoto,§ Hiroshi Takano,∥ Nobuaki Ohguri,∥ Motofumi Matsuda,⊥ Tadatoshi Murota,⊥ Kohei Uosaki,# and Wataru Ueda†

†Catalysis Research Center, Hokkaido University, Kita 21 Nishi 10, Kita-ku, Sapporo 001-0021, Japan

‡Higashifuji Technical Center, Toyota Motor Corporation, 1200, Mishuku, Susono, Shizuoka 410-1193, Japan

§Graduate School of Human and Environmental Studies, Kyoto University, Yoshida-nihonmatsu-cho, Sakyo-ku, Kyoto 606-8501 Japan

∥Fuji Electric Co., Ltd., Yawatakaigandori, Ichihara City, Chiba 290-8511, Japan

⊥Santoku Corporation, 4-14-34, Fukae-kitamachi, Higashinada-ku, Kobe 658-0013, Japan

#International Center for Materials Nanoarchitectonics (WPI-MANA) and Global Research Center for Environment and Energy based on Nanomaterials Science (GREEN), National Institute for Materials Science (NIMS), Namiki 1-1, Tsukuba City, Ibaraki 305-0044, Japan

Supporting Information

ABSTRACT: For the development of a rechargeable metal-air battery, which is expected to become one of the most widely used batteries in the future, slow kinetics of discharging and charging reactions at the air electrode, i.e., oxygen reduction reaction (ORR) and oxygen evolution reaction (OER), respectively, are the most critical problems. Here we report that Ruddlesden−Popper-type layered perovskite, RP-$LaSr_3Fe_3O_{10}$ ($n = 3$), functions as a reversible air electrode catalyst for both ORR and OER at an equilibrium potential of 1.23 V with almost no overpotentials. The function of RP-$LaSr_3Fe_3O_{10}$ as an ORR catalyst was confirmed by using an alkaline fuel cell composed of Pd/$LaSr_3Fe_3O_{10-2x}(OH)_{2x}\cdot H_2O$/RP-$LaSr_3Fe_3O_{10}$ as an open circuit voltage (OCV) of 1.23 V was obtained. RP-$LaSr_3Fe_3O_{10}$ also catalyzed OER at an equilibrium potential of 1.23 V with almost no overpotentials. Reversible ORR and OER are achieved because of the easily removable oxygen present in RP-$LaSr_3Fe_3O_{10}$. Thus, RP-$LaSr_3Fe_3O_{10}$ minimizes efficiency losses caused by reactions during charging and discharging at the air electrode and can be considered to be the ORR/OER electrocatalyst for rechargeable metal-air batteries.

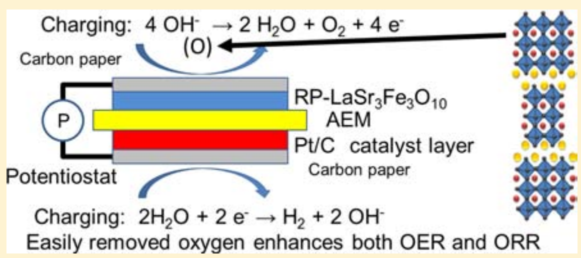

INTRODUCTION

Electric cars are expected to become widely used because of their high energy efficiency. Since the capacitance of a Li-ion rechargeable battery is as low as 200 Wh/kg, rechargeable batteries with higher capacitance are desirable. Although metal-air rechargeable batteries have much higher theoretical capacitance (8228 Wh/kg(Al)) than that of Li-ion rechargeable batteries, calculated on the basis of ref 1 (Figure 1a), they have not been put to practical use.

The cell voltages given are larger than the potential at which aqueous solutions can be electrolyzed; therefore, a non-aqueous or new aprotic solution must be developed. When metal-air batteries are operated under an alkaline condition after developing a new aprotic solution, the discharging reaction would be as follows:

$$\text{metal electrode: } M + nOH^- \rightarrow M(OH)_n + ne^-$$

(M: base metal)

$$\text{air electrode: } 2H_2O + O_2 + 4e^- \rightarrow 4OH^- \quad \text{(ORR)}$$

$$\text{total: } 4M + 2nH_2O + nO_2 \rightarrow 4M(OH)_n$$

The charging reaction is as follows:

$$\text{metal electrode: } M(OH)_n + ne^- \rightarrow M + nOH^-$$

(in aprotic solution)

$$\text{metal electrode: } 2H_2O + 2e^- \rightarrow H_2 + 2OH^-$$

(in aqueous solution)

$$\text{air electrode: } 4OH^- \rightarrow 2H_2O + O_2 + 4e^- \quad \text{(OER)}$$

$$4M(OH)_n \rightarrow 4M + 2nH_2O + nO_2$$

Received: April 8, 2013
Published: June 26, 2013

One of the reasons why metal-air batteries have not been put to practical use is because overpotentials of ORR and OER on the air electrode are generally high. These high overpotentials decrease the efficiencies for discharging and charging reactions.

■ EXPERIMETAL SECTION

Preparation of RP-$LaSr_3Fe_3O_{10}$. Samples of RP-$LaSr_3Fe_3O_{10}$ were synthesized by solid–state reaction. 4.00 g of La_2O_3 (12.4 mmol), 11.07 g of $SrCO_3$ (71.2 mmol), and 5.99 g of Fe_2O_3 (35.6 mmol) were crushed by a planetary ball milling apparatus with a rotational speed of 300 rpm for 60 min. The milled sample was pressed at 30 MPa for 5 min and pelletized into a disk of 20 mm in diameter and 3 mm in thickness. The pellets were calcined in air. Temperature was increased to 1000 °C at a rate of 10 K min^{-1} and then increased to 1400 °C at a rate of 5 K min^{-1}. The temperature was kept at 1400 °C for 3 h. The calcined sample was crushed by a planetary ball milling apparatus with a rotational speed of 300 rpm for 60 min.

Measurement of ORR Activity by a Rotating Disk Electrode (RDE). Solid oxide powders were pressed at 15 MPa for 10 min and calcined at 900 °C for 10 h. The resulting pellets were 3.0 mm in thickness and 10 mm in diameter. An oxide pellet was attached to the diflon cylinder of 10 mm in diameter, and the cylindrical circumference was sealed in a thermal contraction tube. The interior of the cylinder was filled with platinum mesh, and the oxide pellet and an electrode terminal were connected (Figure S1).

ORR activity measurements were carried out by the RDE method using a three-electrode electrochemical jacket cell with a potentiostat (Iviumstat, Ivium Technologies). For comparison, the conventional RDE method with a 46.5 wt % Pt/C (TEC10E50E, Tanaka Kikinzoku) was also used. These powder samples were dispersed in 2.0 mL of distilled water and 3.0 mL of ethanol (Kanto Chemical Co., Inc. Cica-reagent) by sonication (VCX-130PB, Sonic and Materials). Ten μL of dispersed catalyst ink was drop-cast onto a GC electrode (Hokuto Denko). The Pt/C catalyst was set on the electrode with loading of 40 μg cm^{-2}. The catalyst layer on the GC substrate was dried, and then 4 μL of Nafion was drop-cast onto the catalyst layer.

The reference electrode was a commercial alkaline/mercurous oxide reference electrode, and the counter electrode was platinum foil. The rotation speed of the working electrode was 1500 rpm, the speed being controlled by a rotating electrode device (dynamic electrode controller HR-200, Hokuto Denko Corp.). The solutions used were 0.1 M NaOH solutions that were prepared from Direct-Q water (18 MΩ cm) and NaOH (Wako Pure Chemical Industries, Ltd. special grade reagent). All measurements were conducted at 10 mV s^{-1} saturated with O_2 (99.5% Air Water Inc.) at room temperature.

X-ray Absorption Measurement. The powders were pressed into pellets and sintered at 1673 K for 3 h in air. The pellets were annealed at 1073 K for 4 h under oxygen partial pressures of 10^1, 10^2, 10^3, 10^4, or 10^5 Pa. After annealing, the pellets were quenched to 298 K, while the annealing atmosphere was kept constant. After the obtained pellets were pulverized, XRD measurements were performed at 298 K, resulting in the single phase (*I*4/*mmm* space group) for every sample. XAS measurements were performed on BL01B1 at SPring-8 (Hyogo, Japan). The synchrotron radiation X-ray from the storage ring was monochromated by a Si (111) crystal. Fe K-edge XAS spectra were measured at room temperature in transmission mode using two ion chambers. The weighed samples were homogeneously dispersed in dried boron nitride powder to obtain the best XAS spectra. The energy scale was calibrated using Cu and Fe foils. For comparison, single perovskite $La_{0.6}Sr_{0.4}FeO_3$ prepared by a polymerized complex method was used.[2]

Discharging and Charging Reactions Using a Fuel Cell Unit with an AEM. An electrode with a three-layer structure was used to prepare the anode and cathode. For anode catalyst ink, 46.5 wt % Pt/C (TEC10E50E, Tanaka Kikinzoku), water, and 5 wt % anion-exchange resin solution (Tokuyama) were mixed at a weight ratio of 1: 5: 10. The formed catalyst ink was painted on a wet-proofed carbon paper gas diffusion layer (GDL), with a loading amount of 0.5 mg cm^{-2} of Pt. For the air electrode, an RP-$LaSr_3Fe_3O_{10}$ pellet of 1 mm in thickness and 20 mm in diameter was used. The membrane electrode assembly MEA was prepared by pressing two electrodes each on both sides of an anion-exchange membrane (Tokuyama) under 4 MPa for 10 min. The MEA was placed between Au-coated mesh and carbon plates having a gas channel for air electrode side and fuel electrode side, respectively.

I−*V* curves for charging and discharging were obtained at 60 °C and scan rate of 0.9 mA s^{-1} by using an electrical characterization system (HZ-5000, Hokuto Denko Corp.). H_2O-saturated O_2 and H_2 at 60 °C were fed to the air and fuel electrode sides, respectively. The open circuit voltage was 1.23 V, which is almost identical to the theoretical voltage within the experimental error. The inorganic oxide has the possibility of being an ideal electrolyte for a fuel cell.

■ RESULTS AND DISCUSSION

ORR Activity and Structure of Various Metal Oxides. It has been reported that perovskite ABO_3 catalyzed ORR[3−9] and OER[10−16] with redox reaction of B atoms. It was emphasized that electron transfer of antibonding σ e_g and unit occupation of e_g are important.[4,10] One of the formulas for simple perovskite compounds is $LaFeO_3$, where the size of La is larger than that of Fe. La bonds to O in a 12-fold cuboctahedral coordination, while Fe bonds to O in a 6-fold coordination (FeO_6). $LaFeO_3$ consists of rock salt FeO_2 and LaO layers. Each FeO_2 layer is sandwiched by two LaO layers which are shared between this FeO_2 layer and the adjacent FeO_2 layer. Two LaO layers equals 1, since each layer equals one-half. An FeO_2 layer sandwiched by two LaO layers becomes an $LaFeO_3$ perovskite layer. $LaFeO_3$ is composed of infinite perovskite layers of $LaFeO_3$ with bonding (Figure 1b).

Simple perovskite $LaFeO_3$ with excessive (than unit) e_g-filling $(t_{2g})^3(e_g)^2$ for Fe−O_2 is predicted to have low activity for ORR.[4] Low activity of the perovskite $LaFeO_3$ was confirmed by the RDE method (Figure 2). On the other hand, Co in $NaCo_2O_4$ bonds to O in a six-fold coordination (CoO_6), although $NaCo_2O_4$ does not have a perovskite structure. $NaCo_2O_4$ with half e_g-filling $(t_{2g})^5(e_g)^{0.5}$ for Co−O_2 is predicted to have high activity for ORR.[4] $NaCo_2O_4$ has higher ORR activity than that of $LaFeO_3$. It was confirmed that unit e_g-filling is also important for a non-perovskite transition-metal oxide catalyst. Both $LaFeO_3$ and $BaTiO_3$ have the same simple perovskite structures. The perovskite $BaTiO_3$ with no e_g-filling $(t_{2g})^0(e_g)^0$ for Ti−O_2 is predicted to have low activity for ORR. However, the perovskite $BaTiO_3$ has higher activity for ORR than that of $LaFeO_3$. It is well-known that Ti in Ti-silicate, which has high activity for epoxidation of ethylene to ethylene oxide,[17] is reversibly oxidized and reduced. Not only unit e_g-filling but also rapid redox reaction of the transition metal is important.

The onset potential for ORR on Ruddlesden−Popper-type layered perovskite, RP-$LaSr_3Fe_3O_{10}$, was 1.23 V vs RHE, which is an equilibrium potential. RP-$LaSr_3Fe_3O_{10}$ has a perovskite structure in which the size of La or Sr is larger than that of Fe. La or Sr bonds to O in a 12-fold cuboctahedral coordination, while Fe bonds to O in a 6-fold coordination (FeO_6). RP-$LaSr_3Fe_3O_{10}$ has a layered structure. A unit layer is composed of triple perovskite layers of (La or Sr)FeO_3 (n = 3) with an (La or Sr)O layer. Simple perovskite is composed of infinite unit layers of LaFeO (Figure 1b).

For RP-$LaSr_3Fe_3O_{10}$, $Fe^{3.67+}$ has a little excessive e_g-filling $(t_{2g})^3(e_g)^{1.33}$, and it is expected that Fe−O_2 has relatively high activity for ORR. However, the onset potential for ORR is 1.23 V vs RHE, which is the same as the theoretical value. Onset

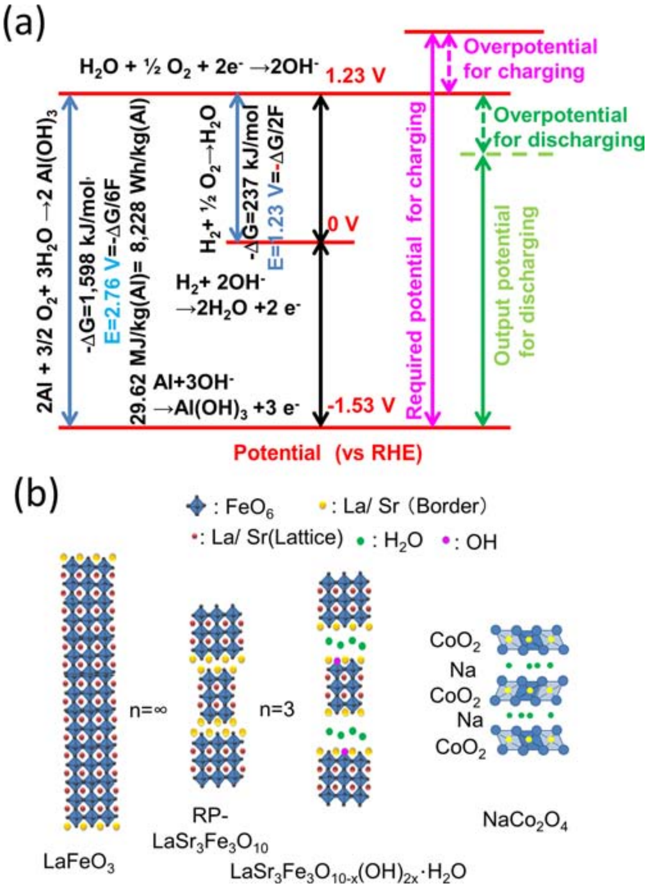

Figure 1. (a) Energy diagram of rechargeable Al-air battery. (b) Structures of various transition metal oxides.

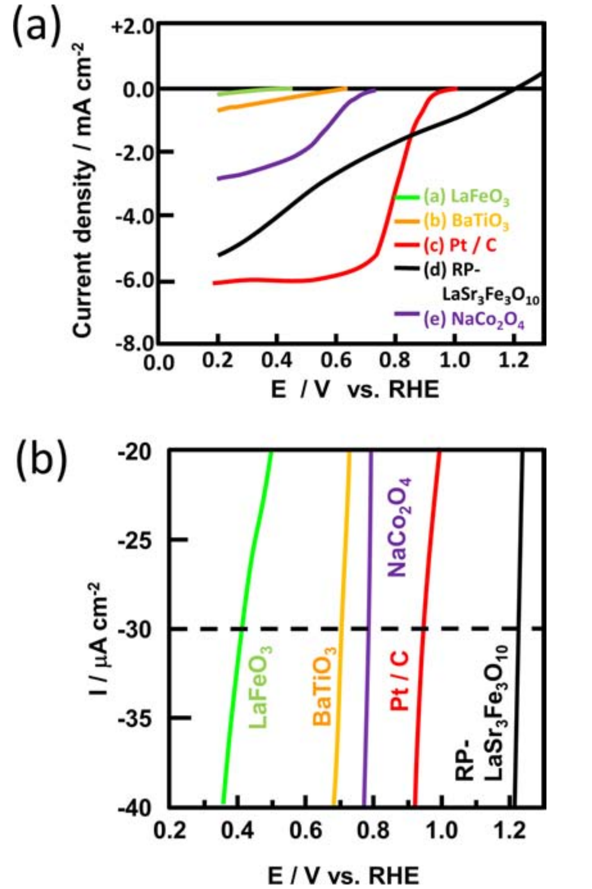

Figure 2. (a) ORR activities of various transition-metal oxides and Pt/C in O_2-sturated 0.1 M NaOH at a scan rate of 10 mV s^{-1} and rotation rate of 1500 rpm. (b) Specific activities of various transition-metal oxides and Pt/C at −30 μA cm^{-2}.

potential obtained by the RDE method suggests that OER occurs at around 1.23 V vs RHE. It is well-known that oxygen present in RP-$LaSr_3Fe_3O_{10}$ is easily removed and that RP-$LaSr_3Fe_3O_{10}$ easily incorporates gas-phase oxygen.[18] With oxygen release and incorporation in perovskite oxides, the formal oxidation number of Fe ions is changed to maintain charge neutral. The change of formal oxidation number in RP-$LaSr_3Fe_3O_{10}$ annealed under various oxygen partial pressures was investigated by X-ray absorption spectroscopy. Figure 3a shows Fe K-edge X-ray absorption near edge structure (XANES) obtained from RP-$LaSr_3Fe_3O_{10}$ annealed under various oxygen partial pressures. The position of the Fe K-absorption edge at about 7123 eV was shifted to lower energy with decreasing oxygen partial pressures. The low-energy shift is interpreted to the reduction of Fe ions as reported in single perovskite $La_{1-x}Sr_xFeO_3$.[19] A decrease in oxygen partial pressures introduces more oxygen vacancies, along with reduction of the Fe oxidation number. The absorption energy shift of Fe K-edge XANES in RP-$LaSr_3Fe_3O_{10}$ is compared with the single perovskite $La_{0.6}Sr_{0.4}FeO_3$. Figure 3b shows the absorption edge energy as a function of oxygen partial pressures for RP-$LaSr_3Fe_3O_{10}$ and $La_{0.6}Sr_{0.4}FeO_3$. The change of absorption edge energy in RP-$LaSr_3Fe_3O_{10}$ is three times larger than that in $La_{0.6}Sr_{0.4}FeO_3$. For $La_{1-x}Sr_xFeO_3$ system, $La_{0.6}Sr_{0.4}FeO_3$ shows easier oxygen vacancy formation with decreasing oxygen partial pressures.[20] Therefore, the redox reaction of Fe ions with oxygen composition change in RP-$LaSr_3Fe_3O_{10}$ is caused more readily than single perovskite oxides. The easy removal of oxygen present in RP-$LaSr_3Fe_3O_{10}$ is considered to enhance ORR activity.

ORR Activity of RP-$LaSr_3Fe_3O_{10}$. A rechargeable metal-air battery for practical use in the future would be a kind of rechargeable alkaline fuel cell. Discharging reaction on the air electrode would be the same as that for an alkaline fuel cell.

$$2H_2O + O_2 + 4e^- \rightarrow 4OH^- \quad E_0 = +1.23\ V(RHE)$$

If RP-$LaSr_3Fe_3O_{10}$ is used as the electrolyte, an oxygen defect would be formed at fuel electrode due to reduction of perovskite oxide. The XRD pattern in Figure 4a suggests that the new component $LaSr_3Fe_3O_{10-2x}(OH)_{2x}\cdot H_2O$ is formed.[21]

$$LaSr_3Fe_3O_{10-x} + (x+1)H_2O$$
$$\rightarrow LaSr_3Fe_3O_{10-2x}(OH)_{2x}\cdot H_2O$$

While thickness of the rock salt (Sr, La)O layer is 2.58 Å for $LaSr_3Fe_3O_{10}$, the thickness was enlarged to 6.15 Å for $LaSr_3Fe_3O_{10-2x}(OH)_{2x}\cdot H_2O$ with intercalation of water and formation of OH group, based on XRD simulation in Figure S4. Low electrical conductivity with high ionic conductivity is needed for a high-performance electrolyte. As shown in Figure 4b, nafion has very low electrical conductivity with maintenance of reasonable ionic conductivity. $LaSr_3Fe_3O_{10-2x}(OH)_{2x}\cdot H_2O$ also has very low electrical conductivity with maintenance of reasonable ionic conductivity because of expansion of thickness of the rock salt layer as mentioned above.

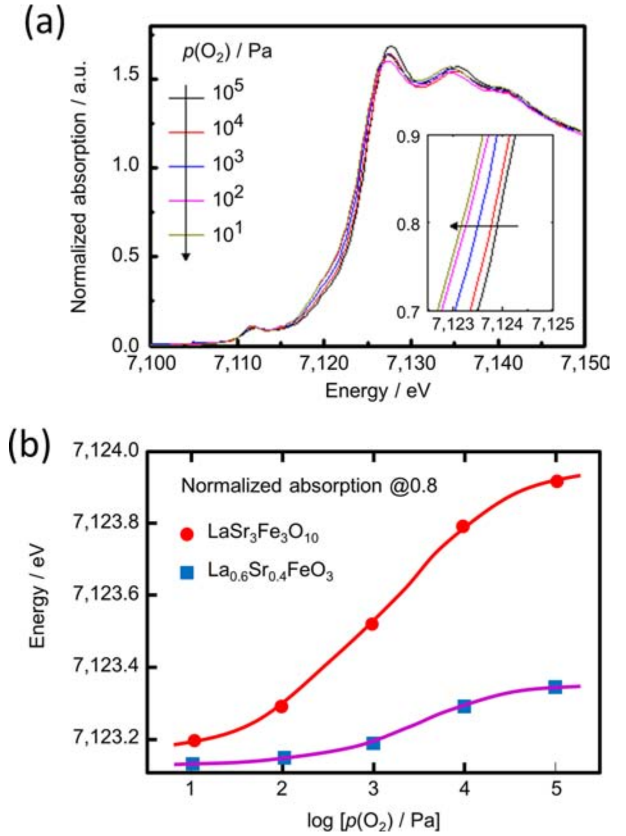

Figure 3. (a) XANES at Fe K-edge of RP-$LaSr_3Fe_3O_{10}$ annealed under various oxygen partial pressures at 1073 K. The inset shows an expanded view around the absorption edge. (b) Fe K-edge absorption energy of RP-$LaSr_3Fe_3O_{10}$ and $La_{0.6}Sr_{0.4}FeO_3$ as a function of the oxygen partial pressure used for annealing. The absorption energy is defined as the intensity of 0.8 in normalized spectra.

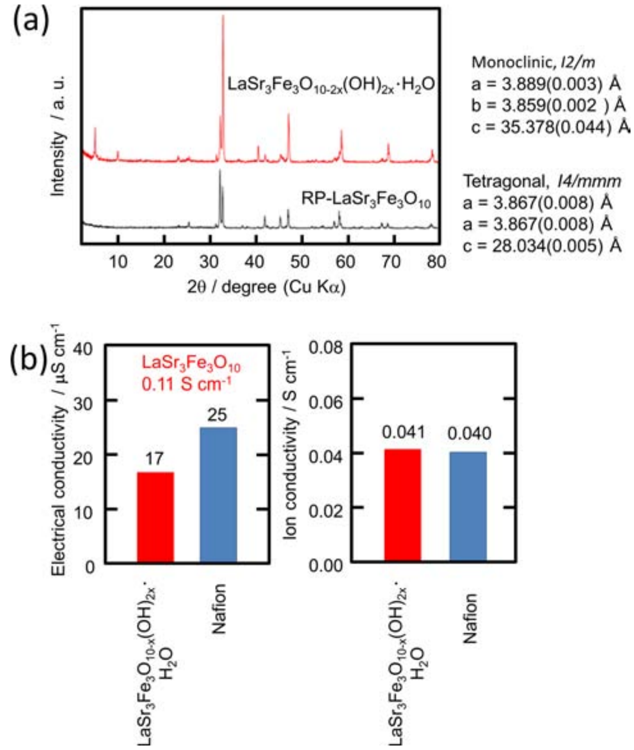

Figure 4. (a) XRD patterns of RP-$LaSr_3Fe_3O_{10}$ and $LaSr_3Fe_3O_{10-2x}(OH)_{2x}\cdot H_2O$. (b) Electrical conductivity and ion conductivity of nafion and $LaSr_3Fe_3O_{10-2x}(OH)_{2x}\cdot H_2O$. These were measured at a cell temperature of 96 °C and electrode temperature of 95 °C.

For fuel cell operation using an H_2 fuel, an MEA used is composed of Pd/$LaSr_3Fe_3O_{10-2x}(OH)_{2x}\cdot H_2O$/RP-$LaSr_3Fe_3O_{10}$ placed between two sheets of carbon paper current collectors. Fuel-cell polarization curves obtained at 95 °C are shown in Figure 5. The current densities exposed to H_2O-saturated O_2 and H_2 at 96 °C on air and fuel electrodes, respectively, are presented. The open circuit voltage is 1.23 V, which is almost identical to the theoretical voltage within the experimental error. Pd, $LaSr_3Fe_3O_{10-2x}(OH)_{2x}\cdot H_2O$, and RP-$LaSr_3Fe_3O_{10}$ functions as a fuel electrode catalyst, an electrolyte, and an air electrode catalyst, respectively. The inorganic oxide has the possibility of being an ideal electrolyte for a fuel cell.

Reduction and water treatment decreased the electrical conductivity by intercalation of water. $LaSr_3Fe_3O_{10-2x}(OH)_{2x}\cdot H_2O$ functions as an electrolyte for OH^- conduction.[22] It has recently been reported that an inorganic oxide containing OH^- functioned as an anion conductor.[23−27] RP-$LaSr_3Fe_3O_{10}$ without intercalation of water with high electrical conductivity functions as a catalyst for oxygen reduction reaction,[28−30] since the fuel cell showed completely theoretical voltage.

OER Activity of RP-$LaSr_3Fe_3O_{10}$. A rechargeable metal-air battery for practical use in the future would be a kind of rechargeable alkaline fuel cell. To evaluate the charging reaction of an alkaline fuel cell, an ORR and OER test unit composed of an anion-exchange membrane (AEM) Tokuyama A201, was constructed (Figure 6a). Polarization curves and current−voltage impressed for charging reaction obtained at 60 °C are

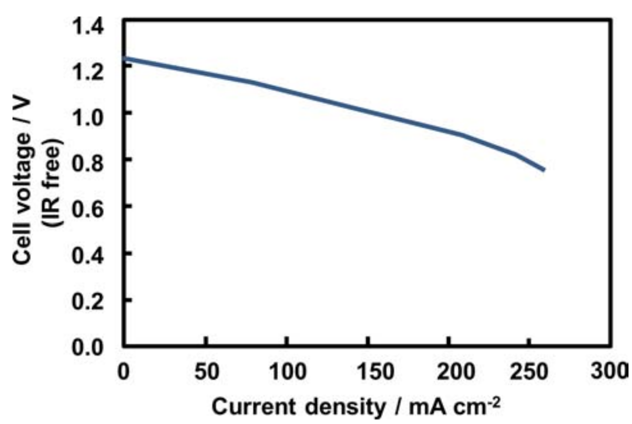

Figure 5. Performance of H_2-fueled solid alkaline inorganic fuel cell, cell voltage versus current densities for Pd/$LaSr_3Fe_3O_{10-2x}(OH)_{2x}\cdot H_2O$/RP-$LaSr_3Fe_3O_{10}$ at 95 °C. Fuel electrode: H_2O-saturated H_2 at 96 °C; air electrode: H_2O-saturated O_2 at 96 °C.

shown in Figure 6b. The current densities exposed to H_2O-saturated O_2 and H_2 at 60 °C at the air and fuel electrodes, respectively, are presented.

$$\text{RP-}LaSr_3Fe_3O_{10} > > LaMnO_3/LaNiO_3 > RuO_2\text{-}IrO_2$$

Results of both ORR and OER testing (Figure 6b) and RDE measurements (Figure 2) show that the activity of RP-$LaSr_3Fe_3O_{10}$ is much higher than the reference values for RuO_2-IrO_2[31] and $LaMnO_3/LaNiO_3$.[32] Since they have large overpotentials for OER and ORR, charging and discharging reactions cause considerable loss of efficiency. Onset potentials

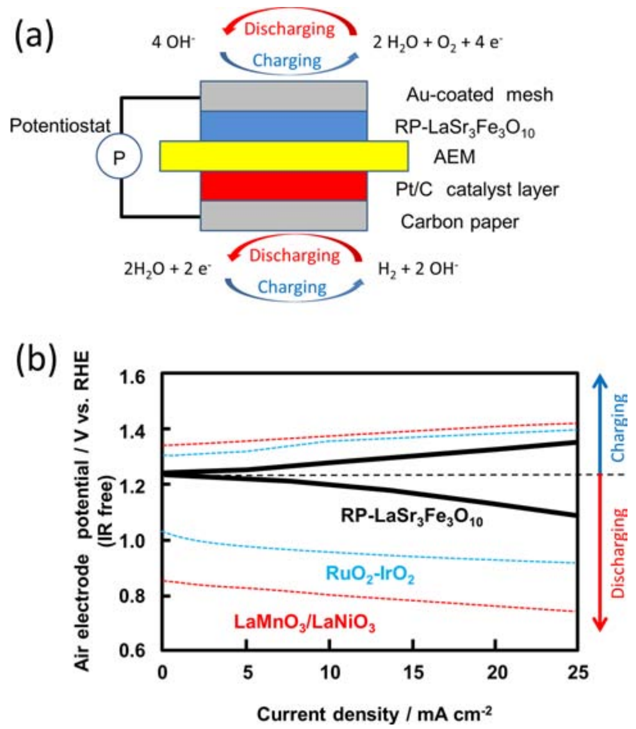

Figure 6. (a) Schematic illustration of ORR and OER test unit with AEM. (b) Performance of ORR and OER of RP-$LaSr_3Fe_3O_{10}$. These were measured at 60 °C. Terminal voltage (V) is almost equivalent to potential of the air electrode (V vs RHE). Reference data, RuO_2-IrO_2[31] and $LaMnO_3$/$LaNiO_3$.[32]

of RuO_2-IrO_2 and $LaMnO_3$/$LaNiO_3$ for OER are around 1.30 and 1.33 V vs RHE, respectively. These results agree with other report obtained by RDE. RP-$LaSr_3Fe_3O_{10}$ functions as a reversible air electrode catalyst for both ORR and OER at an equilibrium potential of 1.23 V with almost no overpotentials. Efficiency loss caused by reactions on the air electrode during charging and discharging becomes the lowest. Oxygen present in RP-$LaSr_3Fe_3O_{10}$ is easily removed, and RP-$LaSr_3Fe_3O_{10}$ incorporates gas-phase oxygen. The easily removable oxygen present in RP-$LaSr_3Fe_3O_{10}$ enhances the activity for OER.

In order to estimate the efficiency loss, we now consider rechargeable Al-air batteries.

$$\mathrm{Al} + 3\mathrm{OH}^- \rightarrow \mathrm{Al(OH)_3} + 3\mathrm{e}^-$$

$$E_0 = -1.50\ \mathrm{V\ vs\ RHE(in\ aprotic\ solution)}$$

$$\mathrm{H_2O} + 1/2\mathrm{O_2} + 2\mathrm{e}^- \rightarrow 2\mathrm{OH}^- \quad E_0 = +1.23\ \mathrm{V\ vs\ RHE}$$

$$\mathrm{total{:}}\ 2\mathrm{Al} + 3/2\mathrm{O_2} + 3\mathrm{H_2O} \rightarrow 2\mathrm{Al(OH)_3}\ E = +2.76\ \mathrm{V}$$

Gibbs free energy for the above $Al(OH)_3$ formation reaction, ΔG, is 1598 kJ/mol.[1] Theoretical voltage for Al-air batteries is 2.76 V (ΔG/6F). Theoretical power density would be 8228 Wh/kg(Al) if rechargeable Al-air batteries are developed in the future after an ideal aprotic solution is obtained. Energy loss on the air electrode was calculated on the basis of overpotentials. Since overpotentials of OER (charging reaction) are 0.07 and 0.10 V for RuO_2-IrO_2 and $LaMnO_3$/$LaNiO_3$, respectively, terminal voltages of charging must be over 2.76 + 0.07 V and 2.76 + 0.10 V for RuO_2-IrO_2 and $LaMnO_3$/$LaNiO_3$, respectively. Therefore, energy losses for charging are 2.5% (0.07 V/(2.76 + 0.07)V) and 3.5% (0.10 V/(2.76 + 0.10)V), respectively. Since overpotentials of ORR (discharging reaction) are 0.20 and 0.37 V for RuO_2-IrO_2 and $LaMnO_3$/$LaNiO_3$, respectively, energy losses for discharging are 7.1% (0.2 V/(2.76 + 0.07)V) and 13% (0.37 V/(2.76 + 0.10)V) for RuO_2-IrO_2 and $LaMnO_3$/$LaNiO_3$, respectively. Totally, 9.6% and 17% of energy are lost on the air electrode during charging and discharging reactions for RuO_2-IrO_2 and $LaMnO_3$/$LaNiO_3$, respectively.

■ CONCLUSIONS

For RP-$LaSr_3Fe_3O_{10}$, overpotentials of OER and ORR are negligible. Reversible ORR and OER are achieved because of the easily removable oxygen present in RP-$LaSr_3Fe_3O_{10}$. Thus, RP-$LaSr_3Fe_3O_{10}$ minimizes efficiency losses at the air electrode and can be considered to be the ORR/OER electrocatalyst for rechargeable metal-air batteries. A negligible portion of energy is expected to be lost on the air electrode by charging and discharging reactions. RP-type layered perovskite is expected to enhance the efficiency of rechargeable Al-air batteries in the future because the easily removal oxygen present in RP-$LaSr_3Fe_3O_{10}$ enhances both OER and ORR.

■ ASSOCIATED CONTENT

Ⓢ Supporting Information

RDE; preparation of Pd/$LaSr_3Fe_3O_{10-2x}(OH)_{2x}{\cdot}H_2O$/RP-$LaSr_3Fe_3O_{10}$ fuel cell, ion and electrical conductivities for nafion and $LaSr_3Fe_3O_{10-2x}(OH)_{2x}{\cdot}H_2O$; identification of the carrier in nafion; AEM and $LaSr_3Fe_3O_{10-2x}(OH)_{2x}{\cdot}H_2O$ to determine conductors in electrolytes; discharging reaction using a fuel cell unit; and stability of RP-$LaSr_3Fe_3O_{10}$. This material is available free of charge via the Internet at http://pubs.acs.org.

■ AUTHOR INFORMATION

Corresponding Author

takeguch@cat.hokudai.ac.jp

Notes

The authors declare no competing financial interest.

■ ACKNOWLEDGMENTS

This study was partly supported by New Energy and Industrial Technology Development Organization (NEDO) of Japan and JST CREST Japan. We thank members of the Technical Division, Catalysis Research Center, Hokkaido University for assistance with manufacturing various reactors for the fuel cell tests. We thank Toyota Motor Corporation for supporting our work. We also thank Prof. Zempachi Ogumi for helpful discussion.

■ REFERENCES

(1) Hemingway, B. S.; Robie, R. A. *Geochim. Cosmochim. Acta* **1977**, *41*, 1402−1404.

(2) Orikasa, Y.; Nakao, T.; Oishi, M.; Ina, T.; Mineshige, A.; Amezawa, K.; Arai, H.; Ogumia, Z.; Uchimoto, Y. *J. Mater. Chem.* **2011**, *21*, 14013−14019.

(3) Suntivich, J.; Gasteiger, H. A.; Yabuuchi, N.; Yang, S.-H. *J. Electrochem. Soc.* **2010**, *157*, B1263−B1268.

(4) Suntivich, J.; Gasteiger, H. A.; Yabuuchi, N.; Nakanishi, H.; Goodenough, J. D.; Yang, S.-H. *Nat. Chem.* **2011**, *3*, 546−550.

(5) Matsuda, M.; Takeguchi, T.; Yamanaka, T.; Takahashi, T.; Ueda, W. *ECS Trans.* **2011**, *35*, 119−124.

(6) Miyazaki, K.; Sugimura, N.; Matsuoka, K.; Iriyama, Y.; Abe, T.; Matsuoka, M.; Ogumi, Z. *J. Power Sources* **2008**, *178*, 683−686.

(7) Tulloch, J.; Donne, S. W. *J. Power Sources* **2009**, *188*, 359−366.

(8) Jörissen, L. *J. Power Sources* **2006**, *155*, 23−32.
(9) Arai, H.; Müller, S.; Haas, O. *J. Electrochem. Soc.* **2000**, *147*, 3584−3591.
(10) Suntivich, J.; May, K. J.; Gasteiger, H. A.; Goodenough, J. B.; Yang, S.-H. *Science* **2011**, *334*, 1383−1385.
(11) Bockris, J. O.; Otagawa, T. *J. Electrochem. Soc.* **1984**, *131*, 290−302.
(12) Bockris, J. O.; Otagawa, T. *J. Phys. Chem.* **1983**, *87*, 2960−2971.
(13) Wattiaux, A.; Grenier, J. C.; Pouchard, M.; Hagenmuller, P. *J. Electrochem. Soc.* **1987**, *134*, 1714−1718.
(14) Matsumoto, Y.; Manabe, H.; Sato, E. *J. Electrochem. Soc.* **1980**, *127*, 811−814.
(15) Matsumoto, Y.; Kurimoto, J.; Sato, E. *J. Electroanal. Chem. Interfacial Electrochem.* **1979**, *102*, 77−83.
(16) Matsumoto, Y.; Sato, E. *Electrochim. Acta* **1979**, *24*, 421−423.
(17) Notari, B. *Catal. Today* **1993**, *18*, 163−172.
(18) Lee, J. Y; Swinnea, J. S.; Steinfink, H.; Reiff, W. M.; Pei, S.; Jorgensen, J. D. *J. Solid State Chem.* **1993**, *103*, 1−15.
(19) Blasco, J.; Aznar, B.; García, J.; Subías, G.; Herrero-Martín, J.; Stankiewicz, J. *Phys. Rev. B* **2008**, *77*, 054107−1−054107−10.
(20) Mizusaki, J.; Yoshihiro, M.; Yamauchi, S.; Fueki, K. *J. Solid State Chem.* **1985**, *58*, 257−266.
(21) Pelloquin, D.; Hadermann, J.; Giot, M.; Caignaert, V.; Michel, C.; Hervieu, M.; Raveau, B. *Chem. Mater.* **2004**, *16*, 1715−1724.
(22) Ueda, W.; Takeguchi, T. WO 2010−007949, 2010.
(23) Tadanaga, K.; Furukawa, Y.; Hayashi, A.; Tatsumisago, M. *Adv. Mater.* **2010**, *22*, 4401−4404.
(24) Furukawa, Y.; Tadanaga, K.; Hayashi, A.; Tatsumisago, M. *Solid State Ionics* **2011**, *192*, 185−187.
(25) Hibino, T.; Shen, Y.; Nishida, M.; Nagao, M. *Angew. Chem., Int. Ed.* **2012**, *51*, 10786−10790.
(26) Tadanaga, K.; Furukawa, Y.; Hayashi, A.; Tatsumisago, M. *J. Electrochem. Soc.* **2012**, *159*, B368−B370.
(27) Watanabe, H.; Takahashi, H.; Takeguchi, T.; Yamanaka, T.; Ueda, W. *ECS Trans.* **2010**, *28*, 147−151.
(28) Watanabe, H.; Takahashi, H.; Takeguchi, T.; Yamanaka, T.; Ueda, W. *ECS Trans.* **2010**, *33*, 1825−1829.
(29) Takahashi, H.; Watanabe, H.; Takeguchi, T.; Yamanaka, T.; Ueda, W. *ECS Trans.* **2011**, *35*, 267−272.
(30) Hibino, T.; Kobayashi, K. *J. Mater. Chem. A* **2013**, *1*, 6934−6941.
(31) Yuasa, M.; Nishida, M.; Kida, T.; Yamazoe, N.; Shimanoe, K. *J. Electrochem. Soc.* **2011**, *158*, A605−A610.
(32) Zhang, Y.; Wang, C.; Wan, N.; Mao, Z. *Int. J. Hydrogen Energy* **2007**, *32*, 400−404.